# A comparative study of electron and positron scattering from chlorobenzene ($C_6H_5Cl$) and chloropentafluorobenzene ($C_6F_5Cl$) molecules

C. Makochekanwa, O. Sueoka, and M. Kimura
*Graduate School of Science and Engineering, Yamaguchi University, Ube, Yamaguchi 755-8611, Japan*

(Received 21 May 2003; accepted 24 September 2003)

Total cross sections (TCSs) for electron and positron scattering from chlorobezene ($C_6H_5Cl$) and chloropentafluorobenzene ($C_6F_5Cl$) molecules have been measured by using the linear transmission time-of-flight method. The impact energies are from 0.4 eV to 1000 eV and 0.2 to 1000 eV for positron and electron impacts, respectively, for scattering from $C_6H_5Cl$ molecules, and 0.8 eV to 600 eV for electron and 0.4 to 600 eV for positron scattering from $C_6F_5Cl$ molecules. Two resonance structures are observed in the $C_6H_5Cl$ electron TCSs at 0.8 eV and 2.5 eV, which merge to the single resonance at 1.6 eV of the $C_6H_6$ molecule. This is an evidence of the splitting of the degenerate $e_{2u}$ orbital of the $C_6H_6$ molecule into two upon substitution of an H atom by the Cl atom. $C_6F_5Cl$ electron TCSs are lower than the positron TCSs at 2–4 eV, otherwise elsewhere, electron TCSs for both $C_6H_5Cl$ and $C_6F_5Cl$ are greater than positron TCSs by a factor of 1–2 at energies up to 30 eV. In the comparative studies of TCSs for $C_6H_5Cl$ with $C_6H_6$ and $C_6F_5Cl$ and $C_6F_6$, the magnitude of TCSs is found to be in the order of the molecular size over all energy ranges, except positron TCSs for $C_6H_5Cl$ and $C_6H_6$ below 600 eV. © *2003 American Institute of Physics.*
[DOI: 10.1063/1.1626115]

## I. INTRODUCTION

In the past few decades, many scientists and engineers have studied processes of electron capture and dissociative electron attachment to halogenated benzenes, alkenes and alkanes, firstly from a basic interest of understanding mechanisms of resonances and consequent dissociation in low-energy electron transport, and secondly from the application point of view that fragmented radical and ionic species of these halogen-containing electronegative gases play an essential role in the plasma processing of microelectronic devices.[1] From experimental as well as theoretical view points, it is very interesting to gain some insights of substitutional effects from haloethylenes, halobenzenes, and halofluorobenzenes as models on unsaturated systems, so that a general principle may be extracted for better understanding of the electronic as well as geometrical molecular-structure effect on electron scattering. Electron capture by these molecules is known to involve the $\pi^*$ molecular orbitals[2–6] and so the substitutional effects on the $\pi^*$ orbital energies should be studied in more detail in conjunction with the collision physics involved. Furthermore, practically, electron capture methods are useful for the detection of halides in chromatographs and other analytical instruments. Besides, dissociative attachment is an important channel for the degradation of halocarbons in the atmosphere in high voltage apparatus. Upon $\gamma$-ray irradiation, organic halides in condensed phases degrade as a result of dissociation arising from capture of thermal secondary electrons that are produced by radiation impinging on a solvent[2] and so any evidence of such degradation would be of important physical implication of the radiation effect.

Whereas a number of studies on electron scattering from halobenzenes, involving electron transmission experiments,[2,3,6] dissociative attachment[7,8] and photoelectron spectra[9] have been carried out, we are not aware of any report on the measurement of total cross sections (TCS) for these molecules except for the low-energy measurements on integral and backward scattering of Lunt *et al.*,[10] in the case of $C_6H_5Cl$. Contrarily, there is no measurement on $C_6F_5Cl$. Neither theoretical nor experimental investigations on positron scattering exist for these two molecules so that the present results are the first systematic studies to be reported.

In this report comparative studies of TCSs for $C_6H_5Cl$ with $C_6H_6$ on one hand, and $C_6F_5Cl$ with $C_6F_6$ on the other are carried out. $C_6H_6$ as a molecule with a large polarizability (69.4 a.u.) and several low-energy negative resonances, has invited a great deal of research interest so that many electron scattering experiments and theoretical works have been carried out to date.[11–13] A number of $C_6F_6$ electron scattering theoretical and experimental works have been carried out including the anion formation cross section experiments of Weik and Illenberger,[14] electron attachment cross section experiments of Marawar *et al.*,[15] and the theoretical and experimental TCSs of Jiang *et al.*[16] and Kasperski *et al.*,[17] respectively. However, there is no earlier TCS studies carried out on positron scattering from $C_6H_6$ and $C_6F_6$, except for our previous work.[18]

In this paper, we report our investigation on total cross section (TCS) measurements from $C_6H_5Cl$ molecules by electron scattering in the impact energy 0.4–1000 eV and by positron scattering in the impact energy of 0.2–1000 eV, and from $C_6F_5Cl$ molecules by electron impact for 0.8–600 eV and by positron impact for 0.4–600 eV. These results are compared with those of $C_6H_6$ and $C_6F_6$,[18] respectively, for the comprehensive understanding of electron and positron scattering from hydrocarbons.

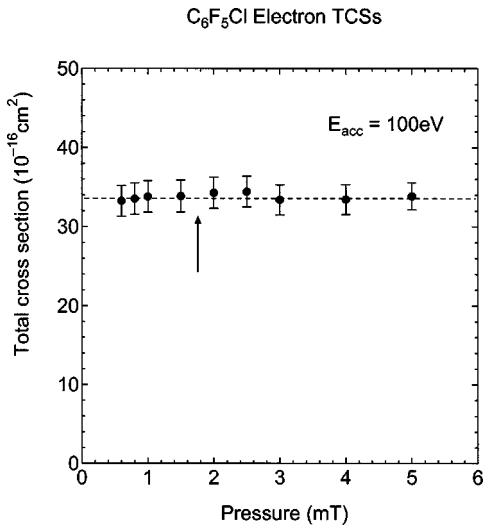


FIG. 1. Electron TCSs for $C_6F_5Cl$ molecules against collision gas pressure. The beam intensity attenuation (Iv/Ig) of 3 used in our TCS measurements for $E_{acc}=100$ eV, is shown by the arrow. Error bars show total uncertainties.

First, electron and positron TCSs for $C_6H_5Cl$ are investigated in comparison with $C_6H_6$ TCSs, and next, the analysis of $C_6F_5Cl$ TCSs in comparison with $C_6F_6$ TCSs follows. Special attention is given here to examining the chlorination effect due to the substitution of the H atom by the Cl atom between $C_6H_5Cl$ with $C_6H_6$ on one hand and $C_6F_5Cl$ with $C_6F_6$ on the other. Last, comparisons of $C_6H_5Cl$, $C_6F_5Cl$, $C_6H_6$, and $C_6F_6$ electron and positron TCSs are discussed in a more systematic manner.

## II. EXPERIMENTAL METHOD

The absolute TCSs for electron and positron scattering from these molecules have been measured using the linear transmission retarding potential time-of-flight (RP–TOF) method in an apparatus setup similar to our previous measurements,[19] and only briefly explained here. An ~80 $\mu$Ci $^{22}$Na radioactive source produces fast positrons, which are converted to a slow beam using an annealed seven-overlapping-layer mesh tungsten moderator set backed at 2100 °C. The energy width of the positron beam was about 2.2 eV. For electron scattering, the slow electrons are produced as secondary electrons emerging from the moderator surfaces after multiple scattering. The electron beam had an energy spread of about 1.4 eV. This beam energy width is different from energy resolution of the experiment which, for instance, is 0.21, 0.23, 0.31, 0.51, 1.0, 2.0, 3.0, 3.0, 4.0 eV at 0.5, 2, 4, 8.0, 20, 50, 100, 250, and 600 eV, respectively.

A pair of Helmholtz coils is used for the canceling off of the effect of the magnetic field due to the earth in the region of the collision cell. The field from these coils is different from the magnetic field parallel to the flight path, due to the solenoid coils, which is applied for beam transportation, as explained below.

Pressure independence of the TCSs was confirmed by carrying out separate experiments at a randomly chosen collision energy value (100 eV) in the current range, and the results are shown in Fig. 1, for $C_6F_5Cl$ electron scattering.

TABLE I. Chlorobenzene ($C_6H_5Cl$) TCSs ($10^{-16}$ cm$^2$) for electron and positron scattering.

| Energy (eV) | Electron | Positron | Energy (eV) | Electron | Positron |
|---|---|---|---|---|---|
| 0.2 | | 19.9±3.0 | 11 | 64.0±3.6 | 37.7±3.4 |
| 0.4 | 44.0±3.1 | 18.0±2.5 | 12 | 61.9±3.5 | 38.7±3.6 |
| 0.6 | 48.1±3.0 | 24.7±3.0 | 13 | 59.8±3.4 | 32.2±3.5 |
| 0.8 | 49.1±3.0 | 25.1±3.0 | 14 | 59.3±3.3 | 35.3±3.2 |
| 1.0 | 48.7±3.0 | 27.3±2.8 | 15 | 57.2±3.3 | 37.3±3.3 |
| 1.2 | 46.5±2.7 | | 16 | 55.9±3.3 | 41.2±3.6 |
| 1.3 | | 30.4±3.1 | 17 | 55.9±3.3 | 35.1±3.3 |
| 1.4 | 45.3±2.7 | | 18 | 55.3±3.3 | 36.7±3.2 |
| 1.6 | 44.0±2.7 | 32.1±3.0 | 19 | 53.5±3.2 | 37.3±3.6 |
| 1.8 | 45.1±2.6 | | 20 | 52.5±3.2 | 33.4±3.2 |
| 1.9 | | 31.4±2.8 | 22 | 50.6±2.9 | 36.3±2.9 |
| 2.0 | 46.3±2.7 | | 25 | 49.6±2.9 | 31.4±3.1 |
| 2.2 | 46.3±2.7 | 31.9±2.8 | 30 | 45.5±2.7 | 34.3±3.0 |
| 2.5 | 47.6±2.7 | 35.5±3.1 | 35 | 44.0±2.6 | |
| 2.8 | 46.8±2.7 | 34.1±3.0 | 40 | 44.9±2.6 | 37.2±3.2 |
| 3.1 | 47.5±2.7 | 33.7±2.9 | 50 | 42.8±2.6 | 29.9±2.8 |
| 3.4 | 47.7±2.7 | 39.3±3.3 | 60 | 38.5±2.2 | 31.1±3.0 |
| 3.7 | 46.6±2.7 | 36.3±3.1 | 70 | 35.7±2.1 | 29.7±2.6 |
| 4.0 | 47.7±2.7 | 36.5±3.0 | 80 | 35.1±2.0 | 29.9±2.7 |
| 4.5 | 50.3±2.9 | 37.1±3.1 | 90 | 32.9±2.0 | 30.0±2.7 |
| 5.0 | 51.3±3.0 | 35.0±2.9 | 100 | 30.8±1.7 | 28.4±2.8 |
| 5.5 | 50.9±3.0 | 39.1±3.1 | 120 | 29.0±1.6 | 27.0±2.8 |
| 6.0 | 54.7±3.2 | 41.8±3.5 | 150 | 27.1±1.5 | 24.4±2.5 |
| 6.5 | 58.2±3.3 | 45.3±3.8 | 200 | 22.6±1.3 | 23.4±2.4 |
| 7.0 | 61.3±3.5 | 44.0±3.5 | 250 | 21.1±1.2 | 18.3±2.0 |
| 7.5 | 65.1±3.8 | 42.3±3.7 | 300 | 18.6±1.0 | 17.0±1.8 |
| 8.0 | 65.8±3.9 | 45.8±3.8 | 400 | 15.9±0.9 | 13.9±1.5 |
| 8.5 | 67.7±3.8 | 43.2±3.8 | 500 | 13.3±0.8 | 12.1±1.3 |
| 9.0 | 66.2±3.9 | 39.3±3.4 | 600 | 11.6±0.6 | 10.1±1.1 |
| 9.5 | 65.3±3.8 | 40.7±3.6 | 800 | 9.5±0.5 | 9.3±0.8 |
| 10 | 64.3±3.6 | 39.7±3.1 | 1000 | 7.7±0.4 | 8.2±0.7 |

The TCS values, $Q_t$, are derived from the Beer–Lambert relation applied as

$$Q_t=(-1/nl)\ln(I_g/I_v), \tag{1}$$

where $I_g$ and $I_v$ refer to the projectile beam intensities transmitted through the collision cell with and without the target gas of number density $n$, respectively. $l$ refers to the effective length of the collision cell and was established by normalizing our measured positron-$N_2$ TCSs to those of the positron-$N_2$ data of Hoffman *et al.*[20] The purpose of this normalization procedure is not only measurement of the effective length, but also for checking the pressure gauge stability. Actually it did not change significantly for each of these measurements. This pressure gauge stability check and the pressure independence of the TCSs highlighted above are an important aspect of these measurements as Kennerly *et al.*[21] also pointed out.

The numerical data for $C_6F_5Cl$ and $C_6H_5Cl$ are shown in Tables I and II, respectively, together with their associated errors determined as follows for both gases. The sum of all the uncertainties was estimated to be 4.4–5.8% and 5.1–11.6% for $C_6F_5Cl$ electron and positron scattering, respectively. As for $C_6H_5Cl$, this sum was 5.5–7.1% and 8.1–14.7% for electron and positron scattering, respectively. This sum of uncertainties is made up of contributions from the <2.0% (<2.1%) for electron and <7.6% (9.8%) for positron beam intensities, $\Delta I/I$, for $C_6F_5Cl$ ($C_6H_5Cl$), where $I$

TABLE II. Chloropentafluorobenzene ($C_6F_5Cl$) TCSs ($10^{-16}$ cm$^2$) for electron and positron scattering.

| Energy (eV) | Electron | Positron | Energy (eV) | Electron | Positron |
|---|---|---|---|---|---|
| 0.4 | | 17.7±2.2 | 11 | 51.2±2.8 | 32.7±2.1 |
| 0.6 | 48.3±3.0 | 20.0±2.1 | 12 | 50.0±2.8 | 31.7±2.0 |
| 0.8 | 46.6±2.8 | 22.1±2.1 | 13 | 51.1±2.8 | 28.7±1.8 |
| 1.0 | 41.3±2.4 | 23.7±2.0 | 14 | 50.6±2.8 | 29.7±2.0 |
| 1.2 | 39.5±22.2 | | 15 | 49.8±2.8 | 31.1±2.2 |
| 1.3 | | 25.4±2.0 | 16 | 49.7±2.8 | 31.8±2.3 |
| 1.4 | 37.1±2.1 | | 17 | 48.8±2.8 | 31.3±2.3 |
| 1.6 | 34.9±2.0 | 25.2±2.0 | 18 | 49.7±2.8 | 32.6±2.4 |
| 1.8 | 33.5±1.9 | | 19 | 48.5±2.8 | 33.0±2.3 |
| 1.9 | | 27.6±2.1 | 20 | 48.0±2.9 | 32.9±2.4 |
| 2.0 | 31.9±1.8 | | 2 | 48.8±2.7 | 33.0±2.1 |
| 2.2 | 29.7±1.7 | 27.2±2.0 | 25 | 47.9±2.7 | 32.6±2.2 |
| 2.5 | 28.3±1.6 | 29.2±2.1 | 30 | 47.4±2.7 | 33.4±2.2 |
| 2.8 | 26.3±1.5 | 29.3±2.1 | 35 | 46.0±2.6 | |
| 3.1 | 25.8±1.5 | 28.9±2.0 | 40 | 44.1±2.5 | 31.0±2.0 |
| 3.4 | 26.6±1.6 | 28.5±2.0 | 50 | 39.5±2.4 | 31.4±2.2 |
| 3.7 | 27.4±1.7 | 29.2±2.0 | 60 | 38.3±2.3 | 30.0±2.1 |
| 4.0 | 28.0±1.7 | 28.9±1.8 | 70 | 37.6±2.1 | 30.0±2.1 |
| 4.5 | 30.5±1.8 | 29.1±1.9 | 80 | 38.2±2.1 | 30.0±2.1 |
| 5.0 | 31.4±1.9 | 30.0±2.0 | 90 | 34.9±2.0 | 29.2±2.1 |
| 5.5 | 35.4±2.0 | 30.0±2.0 | 100 | 34.3±1.9 | 28.5±2.1 |
| 6.0 | 36.1±2.1 | 30.5±2.1 | 120 | 30.7±1.7 | 27.1±2.0 |
| 6.5 | 39.7±2.3 | 30.0±2.0 | 150 | 28.5±1.7 | 25.6±2.0 |
| 7.0 | 41.0±2.4 | 31.3±2.2 | 200 | 25.4±1.5 | 24.0±2.0 |
| 7.5 | 44.7±2.5 | 30.7±2.2 | 250 | 23.5±1.3 | 21.4±1.8 |
| 8.0 | 45.8±2.6 | 30.6±2.2 | 300 | 21.1±1.2 | 21.0±1.7 |
| 8.5 | 48.8±2.7 | 31.8±2.3 | 400 | 18.4±1.1 | 17.0±1.4 |
| 9.0 | 48.3±2.7 | 31.8±2.3 | 500 | 16.3±1.0 | 15.1±1.3 |
| 9.5 | 49.8±2.8 | 31.9±2.4 | 600 | 13.9±0.8 | 14.1±1.2 |
| 10 | 49.2±2.8 | 32.6±2.2 | | | |

refers to $1n(I_g/I_v)$ in Eq. (1). The contribution from the gas density was <3% for both target gas molecules, while that due to the determination of the effective length of the collision cell, $\Delta l/l$, was about 2% for both projectiles.

The parallel magnetic field to the flight path, due to the solenoid coils, is applied for beam transportation. The entrance and exit apertures of the collision cell are very wide, being 3 mm in radius. According to these conditions for this apparatus, the measured raw data are fairly affected by forward scattering effects and a correction for this forward scattering effect is necessary. This correction depends not only on the geometrical conditions including the magnetic field, but also the differential cross section (DCS) data and is carried out using a simulation method[22] similar to that Ma *et al.*[23] Unfortunately because no DCS data is available for any of these two ($C_6H_5Cl$ and $C_6F_5Cl$) molecules, the data presented here could not be corrected for these forward scattering effects. As a result, it is thus possible that the TCSs present here maybe a few percent smaller in magnitude. However, the positions and type of structures observed in our data are not affected by this and are thus credible.

## III. RESULTS AND DISCUSSION

We discuss TCSs for electron and positron impact separately below. Furthermore, detailed comparison, with the

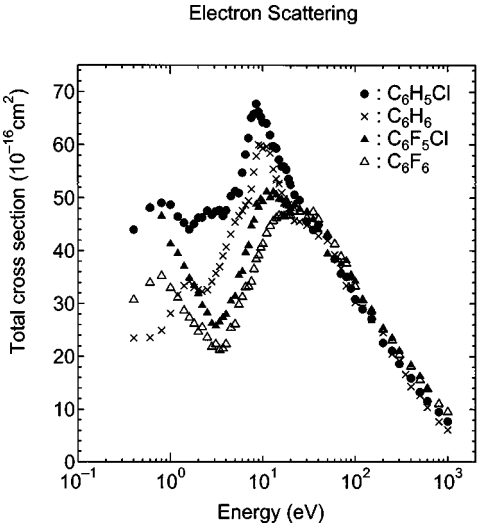


FIG. 2. Electron TCSs for all the molecules.

$C_6H_6$ molecule for $C_6H_5Cl$, and with the $C_6F_6$ molecule for $C_6F_5Cl$, is attempted for a better understanding of the observed structures.

### A. Electron impact

TCSs for scattering from $C_6H_5Cl$ and $C_6F_5Cl$ molecules measured at energies in the ranges 0.4 to 1000 eV for $C_6H_5Cl$, and 0.8 to 600 eV for $C_6F_5Cl$, are shown in Fig. 2, while TCSs for individual molecules are displayed in Figs. 3(a) and 3(b). First we discuss the TCSs shown in Fig. 2, and then proceed to the results for the individual cases in Figs. 3(a) and 3(b). The earlier results for $C_6H_6$ and $C_6F_6$ (Ref. 18) are also included in the figures for comparative discussion.

Taking the $C_6H_6$ molecule as the fundamental parent molecule from which the others are derived, there are some interesting general features in all four sets of TCSs obtained as shown in Fig. 2 and these are summarized as follows: (i) The resonance peak observed at around 10 eV in $C_6H_6$ (Ref. 18 and references therein) is conspicuously seen in all the other molecules. The magnitude of this peak decreases in the order $C_6H_5Cl > C_6H_6 > C_6F_5Cl > C_6F_6$. Besides, the peak position also shifts from lower to higher energies, i.e., it is at

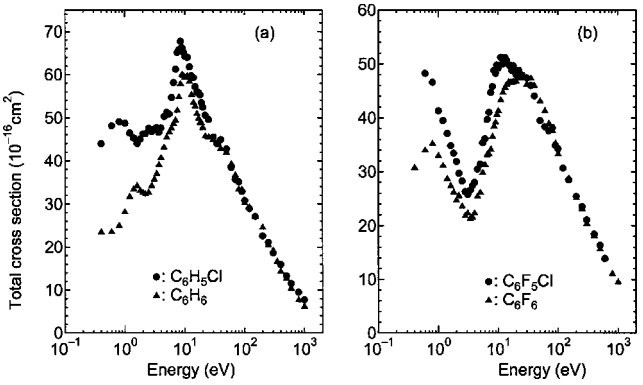


FIG. 3. (a) Electron TCSs for $C_6H_5Cl$ and $C_6H_6$ molecules, (b) electron TCSs for $C_6F_5Cl$ and $C_6F_6$ molecules.

about 8.5, 10, 16, and 25 eV, for $C_6H_5Cl$, $C_6H_6$, $C_6F_5Cl$, and $C_6F_6$, respectively. (ii) A second smaller resonance peak is observed at 1.6 eV in $C_6H_6$ TCSs. Such a low energy peak is also seen in $C_6H_5Cl$ and $C_6F_6$, both at 0.8 eV, but not observed in those of $C_6F_5Cl$. (iii) Below this low energy peak, TCSs for $C_6H_5Cl$, $C_6H_6$, and $C_6F_6$ show decreasing trends. However, $C_6F_5Cl$ TCSs are seen still in an increasing trend below 3 eV. This may correspond to the same resonance peak seen at 0.7 eV for $C_6H_5Cl$. Because $C_6H_5Cl$ and $C_6F_5Cl$ are polar molecules, they are expected to show a rise at much lower energy region, a typical low energy behavior of TCSs for polar molecules. However, in the present energy region, it appears that it has not reached that stage yet. (iv) All the TCSs show decreasing trends above 30 eV and, above a few hundred eV, the magnitude of the TCSs is in the order $C_6F_5Cl > C_6F_6 > C_6H_5Cl > C_6H_6$, which is proportional to the molecular size.

#### 1. $C_6H_5Cl$

In the electronically ground-state $C_6H_6$, the configuration of the six valence electrons in the $\pi$ orbitals shared by the carbon atoms is in $\tilde{x}(a_{2u})^2(e_{1g})^4\,{}^1A_{1g}$ symmetry. The ground state of the resonance temporarily forming $C_6H_6^-$ is expected to be with the configuration $\tilde{x}(a_{2u})^2(e_{1g})^4(e_{2u})^2E_{2u}$.[3] The substitution of an atom or radical destroys the symmetry of the benzene ring, and thus, the degenerate $e_{2u}$ orbital of the benzene molecule is split into two. Apart from this splitting, the Mathur *et al.*[3] transmission spectra of the $C_6H_6$ derivatives are seen to be largely uniform and to resemble to that of the $C_6H_6$ molecules in general features, despite the large changes in symmetry.

As shown in Fig. 3(a) for $C_6H_5Cl$, our observations can be summarized as follows: (i) Two resonance structures are observed at 0.8 eV and 2.5 eV, which should correspond to the single peak of the 1.6 eV $^2E_{2u}$ $C_6H_6$ resonance structure. This is an evidence of the splitting of a peak mentioned above and has been interpreted as being due to the migration of charge in the direction of the $C_6H_6$ ring upon substitution of an H atom by the Cl atom resulting in two resonances, one lying below and the other above the 1.6 eV $^2E_{2u}$ resonance structure of $C_6H_6$.[3] It is worth noting here that though our value of 0.8 eV for the lowest resonance for $C_6H_5Cl$ agrees fairly well with those reported by Mathur *et al.*[3] (0.90 $\pm$0.03 eV), Olthoff *et al.*[2] (0.73 eV) and Lunt *et al.*[10] (0.75 eV), our value for the second resonance structure in the degenerate orbital of 2.5 eV differs from the Mathur *et al.*[3] value of 1.74$\pm$0.04 eV. This discrepancy may be due to the fact that our second resonance peak, quoted as being centered at 2.5 eV, is not as pronounced and sharp as the one at 0.8 eV and could actually be an envelope of resonances existing between 1.7 and 4 eV. Unfortunately, the resolution in our apparatus is not sufficient to resolve its width. Mathur *et al.* also report two other resonances at 3.1 eV and 4.68 $\pm$0.08 eV in their transmission experiments, which are not clearly observed in the present TCSs. The reason for this should mainly be because the cross sections for these resonances must be only about 1–2 Å$^2$, i.e., so small that they cannot be easily identified in the TCSs, whose magnitudes are in the order of 46–50 Å$^2$ at this energy range. (ii) The main resonance peak is observed at 8.5 eV, which should correspond to the 7–13 eV $^2E_{1u}$ main resonance peak for $C_6H_6$. Mathur *et al.* report this peak to be at 8.22 $\pm$0.08 eV, showing a good agreement with our results. (ii) Just like in the case of $C_6H_6$, the TCSs for $C_6H_5Cl$ decrease above this main resonance peak, from $(67.7\pm3.9)\times10^{-16}$ cm$^2$ at 8.5 eV to $(7.7\pm0.4)\times10^{-16}$ cm$^2$ at 1000 eV. (iii) A weak shoulder can be seen at about 40 eV. This is also seen in those of $C_6H_6$. (iv) $C_6H_5Cl$ TCSs are greater than those of $C_6H_6$ particularly below 20–30 eV. The substituted Cl atom is primarily responsible to this consequence through changing the electronic structure and in part, the larger molecular size for $C_6H_5Cl$ than for $C_6H_6$. The general trend that the larger a molecular size becomes, the more likely the corresponding larger TCSs are is a characteristic that has been observed for a number of the polyatomic molecules in this group.[24] The larger TCS is marked below ~10 eV, and the difference is within 15% above 50 eV. Some contributions from the polar nature of $C_6H_5Cl$ to the larger TCSs come in to play below 2 eV. It is obvious that as the impact energy lowers, the incoming electron ''sees'' details of the target character, causing conspicuous differences in various observables from a target to another. As the energy increases, the interaction time becomes shorter hence resulting in a weaker interaction, in which region, the long-range interaction controls the dynamics, and the Born description may be adequate.

#### 2. $C_6F_5Cl$

The results measured over the energy range 0.8–600 eV are shown in Fig. 3(b), together with our previous experimental results of $C_6F_6$.[18] The following interesting features are worth highlighting here. (i) $C_6F_5Cl$ TCSs show a minimum at about 3 eV, just like the $C_6F_6$ TCSs, before showing a rapidly increasing trend at energies below 3 eV. The corresponding $C_6F_6$ TCSs rise below 3 eV but only up to the resonance peak at 0.8 eV, and then are seen decreasing. In electron attachment[25–28] as well as in transmission experiments,[29] the 0.8 eV resonance structure for $C_6F_6$ has also been observed, together with another one at about 0.4 eV that is not observed in our results. It has been explained as due to the resonant capture of the extra electron into the $\pi^*$ orbital, with the formation of a $C_6F_6^-$ anion. The increase in $C_6F_5Cl$ TCSs at this low energy region may come from in part the effect of the permanent dipole moment of this molecule. (ii) The main resonance peak is a broad one observed at 9.5–15 eV, which corresponds to the broad peak at 10–45 eV in $C_6F_6$ TCSs. This broad peak for $C_6F_6$ actually consists of two structures at about 14 eV and 30 eV. The structure at 14 eV has been attributed to the temporary negative-ion resonance formation with subsequent decomposition either through the re-emission of the incident electron or through dissociative electron attachment (DEA) leading to $F^-$, $C_5F_3^-$, and $C_6F_5^-$ fragmented ions.[14,30] Elaborate theoretical studies on resonances from $C_6F_5Cl$ are needed to fully disclose the origin of all resonance peaks observed. It is worth noting here, though, that Bieri *et al.*[31] and Hikida *et al.*[32] did photoelectron spectra measurements of the threshold ioniza-

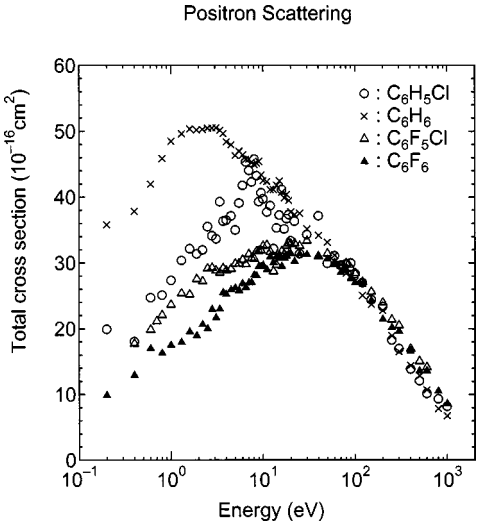


FIG. 4. Positron TCSs for all molecules.

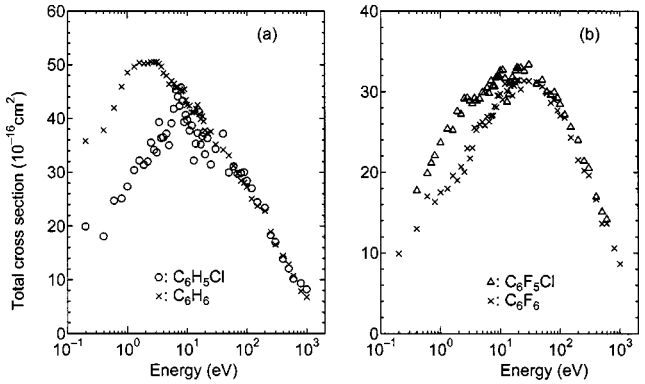


FIG. 5. (a) Positron TCSs for $C_6H_5Cl$ and $C_6H_6$ molecules, (b) positron TCSs for $C_6F_5Cl$ and $C_6F_6$ molecules.

tion energies of the $\tilde{X}\,^2A_2\ (\pi^-)$, $\tilde{B}\,^2B_2\ (\pi^-)$, $\tilde{C}\,^2A_2\ (\pi^-)$ levels, and found corresponding threshold energies to be at 9.9, 12.4, and 12.37 eV for Bieri *et al.* and 9.72, 12.20, and 12.37 eV for Hikida *et al.*, which lie within the current resonance peaks. It is not clear, however, by how much the ionization cross sections from these levels contribute to the TCSs at this energy. (iii) A weak shoulder can also be seen at 25 eV in the current data. (iv) The TCSs decrease beyond this shoulder with almost the same slope as the $C_6F_6$ TCSs. (v) $C_6F_5Cl$ TCSs are greater than $C_6F_6$ TCSs over all the energy ranges, being about 20% greater at all energies below 10 eV and the difference in magnitude decreasing to just about a few percent above 30 eV. This difference is viewed as the chlorination effect resulting from the substitution of the F atom by a Cl atom.

### B. Positron impact

TCSs for positron impact for both $C_6H_5Cl$ and $C_6F_5Cl$ molecules are shown in Fig. 4, along with our previous results for $C_6H_6$ and $C_6F_6$.[18] A few remarks on the TCSs are made as follows: (i) All the TCSs show rising trends from 0.2 eV (0.4 eV for $C_6H_5Cl$) to the main peak, which is centered at about 2 eV for $C_6H_6$, 7.5 eV for $C_6H_5Cl$, and 25 eV for $C_6F_5Cl$ and $C_6F_6$. (ii) This main peak spans from 0.8–5 eV for $C_6H_6$, 6–10 eV for $C_6H_5Cl$, and about 5–80 eV for both $C_6F_5Cl$ and $C_6F_6$ TCSs. (iii) The order of TCSs below 7 eV, is $C_6H_6 > C_6H_5Cl > C_6F_5Cl > C_6F_6$, which differs from the behavior of electron TCSs, described above, in this energy range. (iv) Similar to electron TCSs, the order of magnitude of positron TCSs above a few hundred of eV is found to be in the order of molecular size, i.e., $C_6F_5Cl > C_6F_6 > C_6H_5Cl > C_6H_6$.

#### 1. $C_6H_5Cl$

The positron TCSs measured over the range 0.2–1000 eV are shown in Fig. 5(a), together with those for $C_6H_6$. Special features in these data are analyzed as follows: (i) Because $C_6H_5Cl$ are polar molecules, they are expected to have TCSs that show a rising trend at the lower energy range below a few eV. However, except for the one measured point at 0.2 eV, this trend has not shown up in the current energy range yet. Contrarily, $C_6H_6$ molecules, which are nonpolar, should have little effect from that characteristic at lower energies. (ii) $C_6H_5Cl$ TCSs show a rather sharp and narrower (5–10 eV) peak than $C_6H_6$ (0.7–10 eV). The opening up of the positronium formation channel, with a threshold of 2.26 eV, should be contributing to this peak structure. However, this alone may not fully explain the origin of this rather sharp peak for $C_6H_5Cl$, which is centered at about 7.5 eV. The ionization channel opens up with a threshold of 9.06 eV so that it practically does not contribute to this peak. Therefore, we suspect that this structure, if real, should be due to some strong enhancement from resonance phenomenon. (iii) Both TCSs decrease at higher energies above this main peak with basically the same slope, which is smooth for $C_6H_6$ but shows some less resolved weak structure in the vicinity of 40 eV for $C_6H_5Cl$.

#### 2. $C_6F_5Cl$

Figure 5(b) shows the positron TCSs measured over the range 0.4–600 eV for $C_6F_5Cl$, together with the data of $C_6F_6$. The features seen in these TCSs are summarized as follows: (i) $C_6F_5Cl$ TCSs show the same structural shape as $C_6F_6$ over all the energy range shown here. (ii) However, reflecting somewhat the larger molecular size of $C_6F_5Cl$, $C_6F_5Cl$ TCSs are greater than $C_6F_6$ TCSs over all the energy range; being about 40% greater below 5 eV, less than 10% greater at energies 5–40 eV and this difference in magnitude decreasing with increasing energy above 40 eV, becoming less than a few percent above 200 eV. (iii) $C_6F_5Cl$, like $C_6F_6$ TCSs, shows a decreasing trend below 1 eV. (iv) Again $C_6F_5Cl$, like $C_6F_6$, shows gradually increasing trends, with an unresolved structure at 2–5 eV, up to about 10 eV. The structure at 2–5 eV could be attributed to the opening up of the positronium formation channel, which has a threshold energy of 2.92 eV, just as the structure at about 9–11 eV can be attributed to the ionization channel which opens up at 9.72 eV. (v) An interesting shallow minimum can be seen in both TCSs at about 15 eV. (iv) Both TCSs are seen decreasing above 40 eV with basically the same slope.

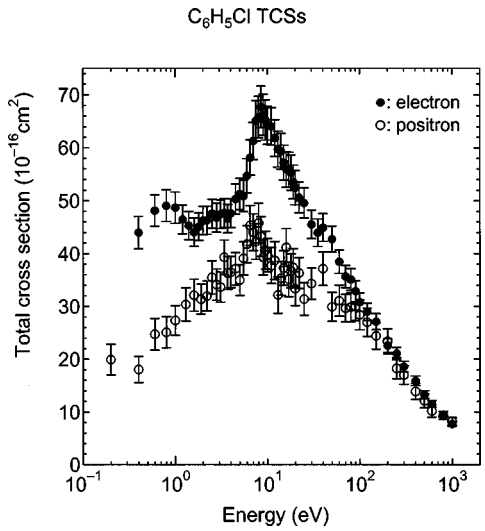


FIG. 6. Electron and positron TCSs for $C_6H_5Cl$ molecules.

Partial-channel cross-section measurements are surely needed for a clear assignment of these structures observed in these positron TCSs of $C_6F_5Cl$, just as is the need also for those of $C_6F_6$.

### C. A comparison of TCSs between electron and positron impacts

TCSs for both electron and positron impacts on $C_6H_5Cl$ and $C_6F_5Cl$ are shown in Figs. 6 and 7. Except for the peculiar behavior of $C_6F_5Cl$ TCSs, where electron TCSs become lower than positron TCSs at 2–4 eV, at low to intermediate energies, the TCSs for electron impact are larger by nearly a factor of 2 due primarily to resonances at energies up to about 30 eV. This characteristic is a clear reflection of the differences in the interaction between the electron and positron with molecules, whereby the existence of shape resonance and attachment phenomena in electron scattering results in increased structure and enhancement of TCSs compared to positron scattering. Below 3 eV, for $C_6F_5Cl$, the TCSs for electron impact show a sharply increasing trend, while TCSs for positron impact display an opposite trend, i.e., a sharply decreasing trend. This low energy behavior in the two TCSs is a very sharp contrast. For $C_6H_5Cl$, on the other hand, TCSs for both electron and positron impact show decreasing trends below 0.8 eV. Positron TCSs seem to show a turn for the rise at 0.2 eV though more measurement points would be necessary below this energy for meaningful analysis. The TCSs for both electron and positron impact, for both $C_6F_5Cl$ and $C_6F_5Cl$, should rise at these low energies due to the strong dipole moments (1.69 D for $C_6H_5Cl$), and if this long-range interaction dominates, then the electron and positron TCSs are expected to behave similarly at these low energies. However, in most of our experiments[24,33] only the TCSs for electron impact show behavior characteristic of polar molecules in this energy range. This clearly suggests that some short-range interaction that is different between electron and positron impacts significantly contributes to the scattering dynamics in this energy range, resulting in the difference in behavior in the two TCSs. As a general trend for both molecules, TCSs for electron and positron impact tend towards merging beyond a few hundred eV.

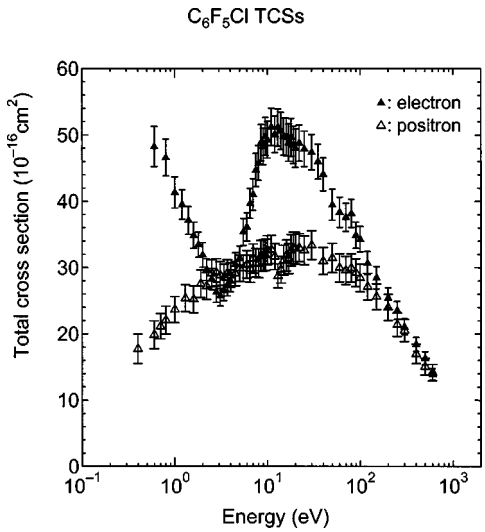


FIG. 7. Electron and positron TCSs for $C_6F_5Cl$ and molecules.

The behavior of $C_6F_5Cl$ TCSs at 2–4 eV, whereby electron TCSs become smaller than their positron counterparts has been observed for some few more molecules studied by our group.[30] It has been suggested that for molecules with a negative quadrupole moment, they should have larger rotational excitation cross sections for positron scattering compared to those in electron counterpart at these energies. Or as a possible alternative interpretation, certainly enhancement due to positron attachment cannot be excluded. If the positron impact can excite a certain type of rovibrational mode or electronic state, then this may lead to specific fragmentation products or excited species, which are grossly different from electron impact. In that case, then the positron impact technique could be usable for selective production of specific fragments or radicals of molecules.

## IV. CONCLUSION

In this report TCS measurements for electron and positron scattering from chlorobenzene ($C_6H_5Cl$) and chloropentafluorobenzene ($C_6F_5Cl$) molecules are presented. We carry out comparative studies of electron and positron TCSs for $C_6H_5Cl$ with $C_6H_6$, and $C_6F_5Cl$ with $C_6F_6$. Virtually no other earlier measurements exist for comparative studies, except for a few fragmentary data for electron impact.

Two resonance structures are observed in the $C_6H_5Cl$ electron TCSs at 0.8 eV and 2.5 eV, corresponding to the 1.6 eV $^2E_{2u}$ $C_6H_6$ resonance structure. $C_6F_5Cl$ electron TCSs show a rising trend below 3 eV, a feature attributed to the polar nature of these molecules. Except for the peculiar 2–4 eV energy range where $C_6F_5Cl$ electron TCSs are lower than positron TCSs, electron TCSs are greater than positron TCSs by a factor of 1–2 at energies up to 30 eV. In the comparative studies of TCSs for $C_6H_5Cl$ with $C_6H_6$ and $C_6F_5Cl$ and $C_6F_6$, molecular size effects have been clearly observed over all energy ranges for all molecular systems except $C_6H_5Cl$ and $C_6H_6$ positron TCSs, below 600 eV. However, the behavior of $C_6F_5Cl$ electron TCSs at 2–4 eV, the other struc-

tures observed at other energy ranges in both electron and positron TCSs for this molecule and, for $C_6H_5Cl$, awaits for more thorough joint theoretical and experimental investigation for better understanding.

## ACKNOWLEDGMENT

This work was supported in part by the Grant-in-Aid from the Ministry of Education, Science, Sport, Culture and Technology, Japan Society for Promotion of Science, Cooperative Research Grant from National Institute for Fusion Science, Japan.

[1] H.-X. Wan, J. H. Moore, and J. A. Tossel, J. Chem. Phys. **94**, 1868 (1991).
[2] J. K. Olthoff, J. A. Tossel, and J. H. Moore, J. Chem. Phys. **83**, 5627 (1985).
[3] D. Mathur and J. B. Hasted, J. Phys. B **9**, L31 (1975).
[4] B. C. Trudell and S. J. W. Price, Can. J. Chem. **57**, 2256 (1979).
[5] L. G. Christophorou, D. L. McCorkle, and J. G. Carter, J. Chem. Phys. **60**, 3779 (1974).
[6] J. R. Frazier, L. G. Christophorou, J. G. Carter, and H. C. Schweinler, J. Chem. Phys. **69**, 3807 (1978).
[7] H. Shimamori, T. Sunagawa, Y. Ogawa, and Y. Tatsumi, Chem. Phys. Lett. **232**, 115 (1995).
[8] H. Shimamori, Y. Tatsumi, and T. Sunagawa, J. Chem. Phys. **99**, 7787 (1993).
[9] M. Mohraz, J. P. Maier, E. Heilbronner, G. Bieri, and R. H. Shiley, J. Electron Spectrosc. Relat. Phenom. **19**, 429 (1980).
[10] S. L. Lunt, D. Field, S. V. Hoffmann, R. J. Gulley, and J.-P. Ziesel, J. Phys. B **32**, 2707 (1999).
[11] R. J. Gulley and S. J. Buckman, J. Phys. B **32**, L405 (1999).
[12] S. Leach, J. Electron Spectrosc. Relat. Phenom. **41**, 427 (1986).
[13] P. D. Burrow, J. A. Michejda, and K. D. Jordan, J. Chem. Phys. **86**, 9 (1987).
[14] F. Weik and E. Illenberg, J. Chem. Phys. **103**, 1406 (1995).
[15] R. W. Marawar, C. W. Walter, K. A. Smith, and F. B. Dunning, J. Chem. Phys. **88**, 2853 (1988).
[16] Y. Jiang, J. Sun, and L. Wan, Phys. Rev. A **62**, 062712 (2000).
[17] G. Kasperski, P. Możejko, and C. Szmytkowski, Z. Phys. D: At., Mol. Clusters **42**, 187 (1997).
[18] C. Makochekanwa, O. Sueoka, and M. Kimura, Phys. Rev. A **68**, 032707 (2003).
[19] O. Sueoka and S. Mori, J. Phys. B **19**, 4035 (1986).
[20] K. R. Hoffman, M. S. Dababneh, Y.-F. Hsieh, W. E. Kauppila, V. Pol, J. H. Smart, and T. S. Stein, Phys. Rev. A **25**, 1393 (1982).
[21] R. E. Kennerly and R. A. Bonham, Phys. Rev. A **17**, 1844 (1978).
[22] A. Hamada and O. Sueoka, J. Phys. B **27**, 5055 (1994).
[23] C. Ma, P. B. Lieschesk, and R. A. Bonham, Rev. Sci. Instrum. **60**, 3661 (1989).
[24] M. Kimura, O. Sueoka, C. Makochekanwa, H. Kawate, and M. Kawada, J. Chem. Phys. **115**, 7442 (2001).
[25] P. G. Datskos, L. G. Christophorou, and J. G. Canter, J. Chem. Phys. **98**, 7875 (1993).
[26] K. S. Gant and L. G. Christophorou, J. Chem. Phys. **65**, 2977 (1976).
[27] H. Shimamori, T. Sunagawa, Y. Ogawa, and Y. Tatsumi, Chem. Phys. Lett. **227**, 609 (1994).
[28] L. G. Christophorou and P. G. Datskos, Int. J. Mass Spectrom. Ion Processes **149/150**, 59 (1995).
[29] J. R. Frazier, L. G. Christophorou, and J. G. Canter, J. Chem. Phys. **69**, 3807 (1978).
[30] G. Kasperski, P. Możejko, and C. Szmytkowski, Z. Phys. D: At., Mol. Clusters **42**, 187 (1997).
[31] G. Bieri, L. Asbrink, and W. V. Niessen, J. Electron Spectrosc. Relat. Phenom. **27**, 129 (1982).
[32] T. Hikida, T. Ibuki, and K. Okada, Chem. Phys. Lett. **292**, 638 (1998).
[33] M. Kimura, O. Sueoka, A. Hamada, and Y. Itikawa, Adv. Chem. Phys. **111**, 537 (1999).